assistance. We also appreciate the outstanding technical suggestions of Drs. R. Schwartz and B. Lubin at the Children's Hospital, Oakland, CA.

References

Alloisio, N., Morle, L., Dorleac, E., Gentilhomme, O., Bachir, D., Guretarni, D., Colonna, P., Bost, M., Zouaoui, Z., Roda, L., Roussel, D., & Delaunay, J. (1985) *Blood 65*, 46–51.
Ames, B. N. (1962) *Methods Enzymol. 8*, 115–118.
Anderson, R. A., & Lovrien, R. E. (1984) *Nature (London) 307*, 655–658.
Anderson, R. A., & Marchesi, V. T. (1985) *Nature (London) 318*, 295–298.
Cohen, C. M. (1983) *Semin. Hematol. 20*, 141–158.
Cohen, C. M., & Korsgren, C. (1980) *Biochem. Biophys. Res. Commun. 97*, 1429–1435.
Cohen, C. M., & Foley, S. F. (1982) *Biochim. Biophys. Acta 688*, 691–701.
Cohen, C. M., & Foley, S. F. (1984) *Biochemistry 23*, 6091–6098.
Cohen, A. M., Liu, S. C., Derick, L. H., & Palek, J. (1986) *Blood 68*, 920–926.
Dixon, M. (1953) *Biochem. J. 55*, 170–171.
Dodge, J. T., Mitchell, C., & Hanahan, D. J. (1963) *Arch. Biochem. Biophys. 100*, 119–130.
Fowler, V., & Taylor, D. L. (1980) *J. Cell Biol. 85*, 361–376.
Goodman, S. R., Yu, J., Whitfield, C. F., Culp, E. N., & Posna, E. J. (1982) *J. Biol. Chem. 257*, 4564–4569.
Granger, B. L., Repasky, E. A., & Lazarides, E. (1982) *J. Cell Biol. 92*, 299–312.
Gutteridge, J. M. C. (1977) *Anal. Biochem. 82*, 76–82.
Leto, T. L., & Marchesi, V. T. (1984) *J. Biol. Chem. 257*, 4603–4608.
Lowry, O. H., Rosenbrough, N. F., Farr, A. L., & Randall, R. J. (1951) *J. Biol. Chem. 193*, 265–275.
Mombers, C. A. M. (1982) Dissertation Thesis, The University of Utrecht.
Mueller, T. J., & Morrison, M. (1981) *Erythrocyte Membranes 2: Recent Clinical and Experimental Advances* (Kruckenberg, W. C., Eaton, J. W., & Brewer, G. J., Eds.) pp 95–112, Alan R. Liss, New York.
O'Farrell, P. (1977) *J. Biol. Chem. 250*, 4007–4021.
Olson, F., Hunt, C. A., Szoka, F. C., Vail, W. J., & Papahadjopoulos, D. (1979) *Biochim. Biophys. Acta 557*, 9–23.
Pasternak, G. R., Anderson, R. A., Leto, T. L., & Marchesi, V. T. (1985) *J. Biol. Chem. 260*, 3676–3683.
Rybicki, A., & Schwartz, R. S. (1985) *J. Cell. Biochem. Suppl. 9B*, 18.
Rybicki, A., Schwartz, R. S., Mueller, T., Wang, W., Chiu, D., & Lubin, B. (1984) *Blood 64 (Suppl. 1)* 112a.
Sato, S. B., & Ohnishi, S. (1983) *Eur. J. Biochem. 130*, 19–25.
Schwartz, R. S., Chiu, D. T. Y., & Lubin, B. (1985) *Curr. Top. Hematol. 5*, 63–112.
Szoka, F., & Papahadjopoulos, P. (1978) *Proc. Natl. Acad. Sci. U.S.A. 75*, 4194–4198.
Szoka, F., & Papahadjopoulos, D. (1980) *Annu. Rev. Biophys. Bioeng. 9*, 467–508.
Tyler, J. M., & Branton, D. (1980) *J. Ultrastruct. Res. 71*, 95–102.
Tyler, J. M., Hargreaves, W. R., & Branton, D. (1979) *Proc. Natl. Acad. Sci. U.S.A. 76*, 5192–5196.
Tyler, J. M., Reinhardt, B. N., & Branton, D. (1980) *J. Biol. Chem. 255*, 7034–7039.
Ungewickell, E., Bennet, P. M., Calvert, R., Ohanian, V., & Gratzer, W. B. (1979) *Nature (London) 280*, 811–814.
Wilschut, J., Duzgunes, N., Fraley, R., & Papahadjopoulos, P. (1980) *Biochemistry 19*, 6011–6021.

Interaction of Sperm Histone Variants and Linker DNA during Spermiogenesis in the Sea Urchin†

George R. Green‡ and Dominic L. Poccia*
Department of Biology, Amherst College, Amherst, Massachusetts 01002
Received August 7, 1987; Revised Manuscript Received September 29, 1987

ABSTRACT: Several physical properties of sea urchin spermatid chromatin, which contains phosphorylated Sp H1 and Sp H2B histone variants, and mature sperm chromatin, in which these histones are dephosphorylated, were compared. Density, thermal stability, average nucleosomal repeat length, and resistance to micrococcal nuclease digestion are all increased in mature sperm relative to spermatid chromatin. Since the chromatins are identical in histone variant subtypes, the altered physical properties are not a consequence of changes in histone primary structure during spermiogenesis. The data are interpreted to mean that dephosphorylation of the N-terminal regions of Sp H1 and Sp H2B in late spermatid nuclei permits strong ionic binding of these highly basic regions to the extended linker, stabilizing the highly condensed structure of sperm chromatin.

While conservation of histone amino acid sequence and structure is the general rule for eukaryotic chromosomes, many exceptions occur in sperm cells of animal and plant species (Poccia, 1986). In extreme instances, such as protamine-containing sperm of trout and mammals, nucleosomal structure is abandoned, and histones are replaced by various highly basic proteins. While such proteins are often assumed to be involved in chromatin condensation or packing, in most cases little is known about how their structural features contribute to the

† Supported by NIH Grant HD 12982.
* Correspondence should be addressed to this author.
‡ Present address: Biology Department, Mount Holyoke College, South Hadley, MA 01075.

0006-2960/88/0427-0619$01.50/0

special properties of sperm chromatin or how their interactions with DNA are modulated during differentiation of the spermatid.

The chromatin of the sea urchin spermatozoon is strikingly different from somatic chromatin in several respects. Sea urchin sperm chromatin has the longest known average nucleosomal repeat length, a consequence of its long linker (Spadafora et al., 1976; Simpson & Bergman, 1980). The chromatin is packed at nearly maximal density, approaching or exceeding the DNA concentration of mitotic chromosomes or 30-nm interphase fibers (Green & Poccia, 1985). It is exceptionally stable toward thermal or ionic denaturation (Ozaki, 1971; Simpson & Bergman, 1980). Although sea urchin sperm chromatin contains histones rather than protamines, two of these are "sperm-specific" histone variants (Sp H1 and Sp H2B).[1] They are larger than their embryonic counterparts, mostly by virtue of highly basic N-terminal extensions (arms) which consist predominantly of simple repeating tetra- or pentapeptides (Strickland et al., 1978, 1980). The tetra- and pentapeptides are related in sequence to one another, possessing two basic amino acids adjacent to the dipeptide serine-proline (Poccia, 1987). The arms have been postulated to play a role in maintaining or stabilizing the structure of the highly condensed sperm nucleus (Strickland et al., 1978; Green & Poccia, 1985). Excluding the arms, the remainder of each Sp histone has sequence features very similar to those of somatic histones (Poccia, 1987).

The Sp histones are actually testis-specific rather than sperm-specific. Their mRNAs are expressed exclusively in the testis (Busslinger & Barberis, 1985; Lieber et al., 1986; Lai & Childs, 1986). The proteins, in their phosphorylated forms (designated N and O/P), appear in chromatin of the male germ cell lineage prior to spermatid differentiation (spermiogenesis); they are dephosphorylated late in spermiogenesis, forming Sp H1 and Sp H2B, the proteins found in the mature sperm (Poccia et al., 1987). These observations raise the question of whether the unusual features of sperm chromatin structure are acquired when the Sp histone variants replace somatic histones or when they become dephosphorylated.

Dephosphorylation of sperm nuclear proteins also occurs during spermiogenesis in trout and winter flounder (Louie & Dixon, 1972; Kennedy & Davies, 1982). However, these events differ from those observed during sea urchin spermiogenesis in two important ways: (1) During trout and winter flounder spermiogenesis, histones are replaced by protamines or protamine-like proteins; histones are retained throughout sea urchin spermatogenesis; (2) dephosphorylation of trout and winter flounder nuclear proteins occurs in parallel with chromatin condensation, whereas dephosphorylation of N and O/P occurs after most chromatin condensation has occurred (Poccia et al., 1987; Simpson & Poccia, 1987).

We have suggested that multiple phosphorylations of the N-terminal arms of N and O/P decrease their affinities for the DNA backbone and allow the histones to function as typical histones throughout spermatogenesis. Dephosphorylation late in spermiogenesis would then allow the basic arms to bind DNA in the linker region, cross-linking and stabilizing the highly condensed sperm nucleus (Poccia et al., 1987). Sp H1 and Sp H2B are rephosphorylated immediately after fertilization; we have proposed that this event helps to destabilize the sperm nucleus, allowing the chromatin to decondense during formation of the male pronucleus (Green & Poccia, 1985; Poccia, 1987).

In an attempt to understand the role of the terminal arms of Sp histones in the structure of sperm chromatin, we have isolated by density gradient centrifugation a population of male germ line nuclei essentially free of mature sperm nuclei and compared several physical properties of chromatin from these nuclei with chromatin from shed sperm. The results demonstrate a substantial increase in average nucleosomal repeat length during spermiogenesis without change in histone variant subtypes. This change is accompanied by increased linker resistance to micrococcal nuclease digestion and increased thermal stability of the chromatin and is interpreted to reflect in large part the binding of dephosphorylated N-terminal arms of Sp H1 and Sp H2B to the extra linker DNA.

Materials and Methods

Preparation of Sperm and Spermatid Nuclei. Sea urchins (*Stronglyocentrotus purpuratus*) obtained in late September from Marinus, Inc. (Westchester, CA), were injected with 0.5 M KCl. A male was chosen which shed a small amount of sperm and which, upon dissection, contained well-developed gonads. Shed sperm were collected and stored on ice. All subsequent steps were at 4 °C.

One gonad was immersed in 20 mL of NB buffer (0.15 M NaCl, 1 mM phenylmethylenesulfonyl fluoride, and 10 mM Tris-HCl, pH 8.0) and gently teased for 5 min to release sperm. The gonad was then placed in 40 mL of NB buffer containing 0.5% TX-100 and dispersed with a polypropylene disposable transfer pipet. This procedure lysed the dispersed cells, as judged by phase microscopy. The nuclear suspension was passed through a 50-μm Nitex screen to remove connective tissue and then centrifuged at 3000g for 5 min to pellet the nuclei. The nuclei were suspended in 25 mL of NB buffer, layered over 15 mL of NB buffer made 10% in sucrose by addition of dry sucrose, and centrifuged at 3000g for 5 min.

Purification of Sperm and Spermatid Nuclei by Centrifugation in Percoll. Percoll gradients (25 mL) were generated from 80% Percoll (Pharmacia) in NB buffer by centrifugation in a Beckman Type 50.2 fixed-angle rotor at 20 000 rpm for 30 min. Gradient densities were determined by inclusion of latex marker beads (Pharmacia).

Gonadal nuclei were suspended in 5 mL of NB buffer using a plastic transfer pipet. The suspension was filtered through 50-μm Nitex, and 2.5-mL portions were layered onto two 25-mL Percoll gradients. Gradients were centrifuged at 15 000 rpm for 20 min in an SW 28 rotor. Gradients were collected from the top as 5-mL fractions while the turbidity of the gradient was measured continuously at 540 nm using a Beckman spectrophotometer equipped with a flow cell. Two volumes of NB buffer were added to each fraction and the nuclei collected by centrifugation at 3000g for 5 min. The nuclei were suspended in 3 mL of NB buffer, repelleted, and suspended in 200 μL of NB buffer. The fractions were examined by phase microscopy to identify those enriched in spermatid nuclei and freed of sperm nuclei. Fractions III met these criteria and were pooled and designated "spermatid nuclei".

Sperm nuclei were prepared from semen as above except that, after suspending the sperm cells in NB buffer containing 0.5% TX-100, tails were removed by brief sonication in a small bath sonicator (Poccia & Green, 1986). The sperm nuclei banded tightly near the bottom of the gradients, and fractions

[1] Abbreviations: Sp H1, sperm histone H1 variant; Sp H2B, sperm histone H2B variant; NB buffer, 0.15 M NaCl, 1 mM phenylmethylenesulfonyl fluoride, and 10 mM Tris-HCl, pH 8.0; TX-100, Triton X-100; AUT, acid, urea, and TX-100; SDS, sodium dodecyl sulfate; bp, base pair(s); Tris-HCl, tris(hydroxymethyl)aminomethane hydrochloride; EDTA, ethylenediaminetetraacetic acid; HMG, high mobility group.

V were collected from two gradients, pooled, and designated "sperm nuclei".

Characterization of Percoll-Purified Sperm and Spermatid Nuclei. Nuclei obtained from Percoll gradients were stained with acridine orange and photographed using fluorescence and phase optics. The nuclei were categorized according to previously established criteria (Simpson & Poccia, 1987) and counted. Photographs of 5 separate fields of each sample (70–200 nuclei each) were counted for major nuclear types and the means and standard deviations of the counts calculated. Samples of the nuclei were mixed with protamine extraction buffer and analyzed by two-dimensional polyacrylamide gel electrophoresis as previously described (Poccia & Green, 1986). The gels contained acetic acid, 6 M urea, and TX-100 in the first dimension and SDS in the second dimension.

Micrococcal Nuclease Digestion. Nuclei were suspended in 0.25 mM EDTA (pH 8.0) and placed on ice for 1 h. The swollen chromatin was pelleted by centrifugation at 10000*g* for 10 min, then resuspended in 0.25 mM EDTA, and incubated on ice for 1 h. The chromatin was adjusted with 0.25 mM EDTA to approximately 10 mg of DNA/mL, determined by dissolving an aliquot in 1% SDS and measuring the absorbance at 260 nm, assuming 1 absorbance unit at 260 nm represented 40 μg of DNA. A sample of the chromatin, containing approximately 100 μg of DNA, was removed for thermal denaturation (see below). $CaCl_2$ was added to a final concentration of 1 mM, and an undigested sample was removed from the chromatin suspension. The suspension was brought to 22 °C, micrococcal nuclease (Sigma Chemical Co.) was added to a concentration of 5 μg/mL, and samples were taken at 2-, 4-, 8-, and 16-min intervals. Immediately after each sample was taken, EDTA and SDS were added to 5.0 mM and 1.0%, respectively, and the samples were placed on ice.

DNA Purification, Acid Solubility, and Agarose Gel Electrophoresis. DNA was purified and analyzed on 2% agarose gels as previously described (Poccia et al., 1984). Migration distances for dimers to pentamers were entered into a computer program, and their sizes in base pairs were determined from a calibration curve made from ϕX174 DNA restricted with *Hae*III. Sizes of the multimer bands were plotted vs multimer number, and the slope of the resulting line was used to determine the nucleosome repeat. The degree of DNA digestion was determined by mixing 5 μL of the digested samples, after addition of SDS and EDTA, with 0.5 mL of 0.5 M $HClO_4$ and placing the mixture on ice for 1 h to precipitate undigested DNA. The insoluble material was pelleted by centrifugation at 10000*g* for 5 min, resuspended in 0.5 mL of 0.5 M $HClO_4$, and centrifuged as above. The supernatants were combined, and the amount of acid-soluble DNA was determined by measuring the absorbance at 260 nm. The acid-insoluble DNA was hydrolyzed in 1.0 mL of 1.5 M $HClO_4$ at 70 °C for 1 h, insoluble material was removed by centrifugation, and the amount of acid-insoluble DNA was determined by the absorbance at 260 nm. The percent of DNA digested by micrococcal nuclease was expressed as 100[($HClO_4$-soluble DNA)/($HClO_4$-soluble + $HClO_4$-insoluble DNA)].

Thermal Denaturation. Samples of sperm and spermatid chromatins, containing approximately 100 μg of DNA, were suspended in 1 mL of 0.25 mM EDTA by drawing the suspension through a 20-guage hypodermic syringe 10 times and dialyzed overnight against 3 L of 0.25 mM EDTA. Insoluble material was removed by centrifugation at 3000*g*, and the samples were adjusted to absorbances of 0.5 at 260 nm. The chromatin was denatured in a Gilford spectrophotometer equipped with a thermally jacketed cuvette chamber and a chart recorder with a sensitive slide wire, as previously described (Green et al., 1981).

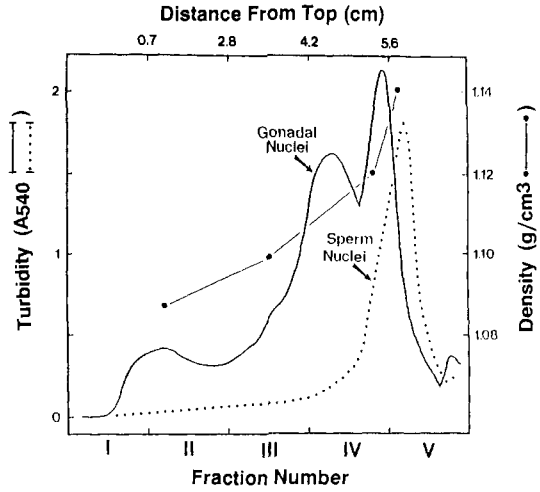

FIGURE 1: Purification of sperm and spermatid nuclei by centrifugation in Percoll gradients. Sperm (···) and gonadal (—) nuclei were centrifuged in Percoll gradients which were removed from the top, passed through a flow cell to monitor turbidity at 540 nm, and collected as 5.0-mL fractions. Gradient densities (●) were determined by inclusion of latex marker beads. Fractions from two identical gradients containing sperm nuclei and from two identical gradients containing spermatid nuclei were pooled, and the nuclei were washed free of Percoll and examined by phase-contrast microscopy. Fraction V from the sperm gradient and fraction III from the gonadal gradient were designated sperm and spermatid nuclei, respectively, and were used in subsequent experiments.

RESULTS

Isolation of Sperm and Spermatid Nuclei. Although animals of differing degrees of maturity can be used to enrich gonadal nuclear isolates for various stages, some mature sperm nuclei are almost always present (Poccia et al., 1987). In this study, we separated spermatid nuclei from sperm nuclei by centrifugation of nuclear suspensions to equilibrium in Percoll gradients (Figure 1). The method exploits the high density of sperm nuclei, which band sharply with a peak at 1.142 g/cm^3. When testicular nuclei were centrifuged in Percoll, fractions III, IV, and V, with densities ranging from 1.095 to 1.145 g/cm^3, contained spermatid nuclei which generally decreased in diameter with increasing density (data not shown). Since many sperm nuclei contaminated fractions IV and V, fraction III, which contained few mature sperm nuclei, was used (1.095–1.107 g/cm^3). This fraction was designated "spermatid nuclei".

Characterization of Percoll-Purified Sperm and Spermatid Nuclei. Gradient-purified nuclei were obtained from shed sperm and consisted of >99% sperm nuclei (Figure 2a,b). Sp H1 and Sp H2B histones from these nuclei were entirely in the mature or unphosphorylated form (Figure 2e) [see Poccia et al. (1987)]. Extremely low levels of non-histone proteins were present in the overloaded gel.

Nuclei from the spermatid fraction are shown in Figure 2c,d. The nuclei were a mixed population of spermatid nuclei (ca. 85% early spermatid) with small numbers of spermatocyte and sperm nuclei and others of undetermined origin. Mature sperm nuclei contributed 4% ± 2%, mid to late spermatid nuclei 5% ± 2%, and pre-spermatid, damaged, or unclassified nuclei 5% ± 1%. Nuclei from the spermatid fraction contained, as representatives of the H1 and H2B classes, almost entirely Sp H1 and Sp H2B histones in the phosphorylated forms, referred

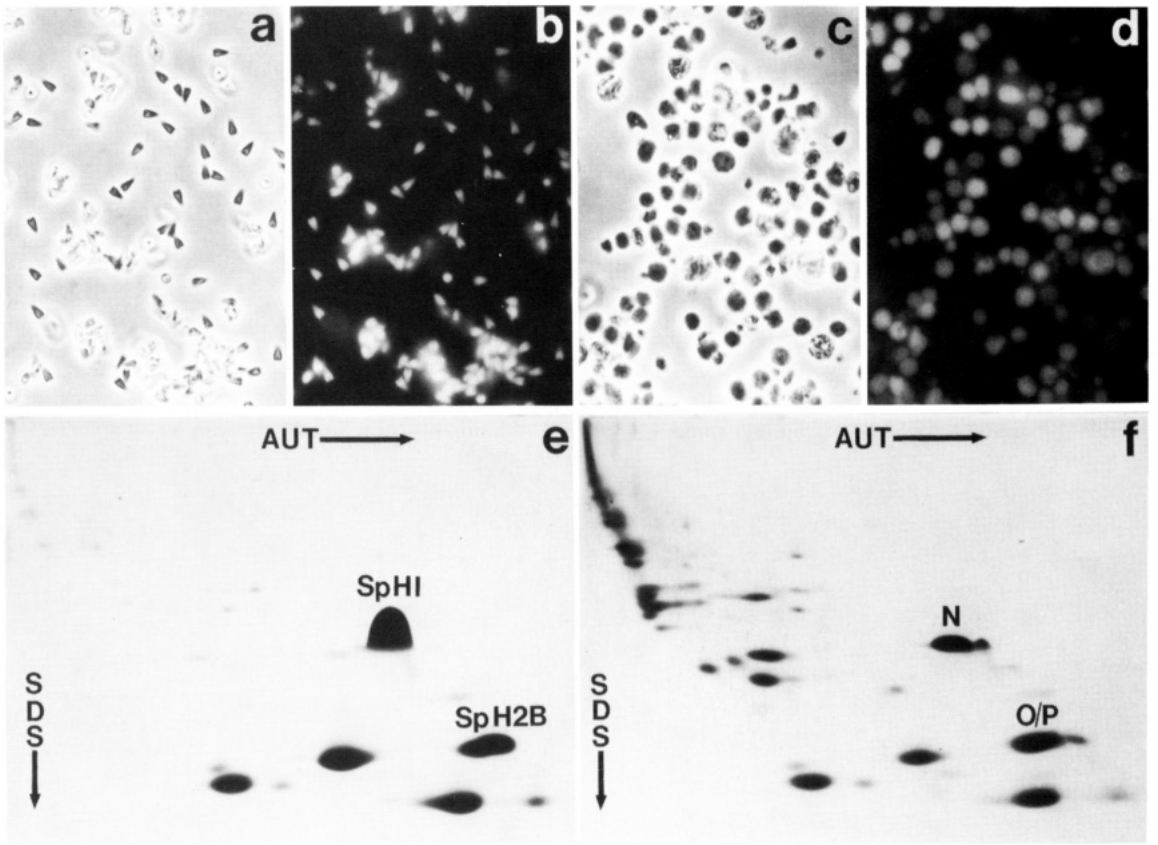

FIGURE 2: Characterization of nuclei and nuclear proteins from Percoll-purified sperm and spermatid nuclei. Samples of sperm and spermatid nuclei were stained with acridine orange and photographed with phase (panels a and c, respectively) and fluorescence (panels b and d, respectively) optics. Samples of Percoll-purified nuclei were mixed with protamine extraction buffer and analyzed by two-dimensional polyacrylamide gel electrophoresis (panels e and f, respectively; acid–urea–Triton X-100 in the first dimension and sodium dodecyl sulfate in the second dimension). The gels were stained with Coomassie Blue R-250.

to as N and O/P, respectively (Figure 2f; Green & Poccia, 1985; Poccia et al., 1987). Small amounts of Sp H1 and Sp H2B in this fraction probably result from the low level of contamination by mature sperm. Barely detectable levels of somatic histone variants are seen.

In contrast to the sperm fraction, a number of proteins which did not comigrate with core or H1 histones were present. These proteins may be divided into two groups: a heterogeneous group of relatively large proteins, which appear in the upper left diagonal of the gel, and a small number of prominent, low molecular weight proteins, which migrate to the left of the major histone species. From their positions in the gel, the low molecular weight proteins may include ubiquitinated forms of H2A, core histone dimers, HMG proteins, or other non-histone proteins.

Micrococcal Nuclease Digestion. Micrococcal nuclease was used as a probe of linker state in spermatid and sperm chromatin. Each chromatin was adjusted to 10 mg of DNA/mL and digested with an equal amount of micrococcal nuclease. The release of DNA soluble in 0.5 M $HClO_4$ is shown in Figure 3a, and the large DNA fragments produced, resolved by agarose gel electrophoresis, are shown in Figure 3b.

These analyses provide two estimates of the relative rates of digestion of the two chromatins with micrococcal nuclease. At each time point, 1.5–2 times as much $HClO_4$-soluble DNA was released in the spermatid chromatin compared to sperm (Figure 3a). As evaluated by the production of equivalent distributions of larger multimer sizes (Figure 3b), the spermatid digest at 4 min (lane 11) lies between sperm digests of 8 and 16 min (lanes 5 and 6); the 2-min digest (lane 10) lies between the 4- and 8-min sperm digests (lanes 4 and 5). Thus, for a single DNA duplex cut, spermatid linker is attacked 2–4 times as fast as sperm linker. The rate of digestion of spermatid chromatin with respect to sperm chromatin is similar to rates determined for typical sea urchin embryo chromatins (Arceci & Gross, 1980).

The nucleosomal repeat lengths for sperm and spermatid chromatins were determined for different degrees of digestion (Figure 3a). Nucleosomal repeat lengths for each chromatin decreased slightly with increasing digestion, reaching plateaus at higher times of digestion. The maximal difference in repeat length for the two chromatins was ca. 20 bp. For chromatins digested to approximately equal degrees (sperm, lane 5, and spermatid, lane 11, in Figure 3b), the repeat lengths were 234 and 250 bp, respectively. The repeat length for spermatid chromatin is similar to that of late embryos previously determined (Keichline & Wasserman, 1977; Arceci & Gross, 1980; Savič et al., 1981).

The most highly digested chromatins produced monosomal DNA fragments ranging from approximately 150 to 250 bp for sperm and 150–236 bp for spermatid (Figure 3b, lanes 6 and 13), ranges extending from approximately core DNA length to one complete repeat length in each case. For samples digested to approximately the same degree (lanes 5 and 6 for sperm vs lane 11 for spermatid chromatin), the distribution of monomer DNA ranged evenly over the size range for sperm monosomes, in contrast to spermatid monosomes, which were predominantly of sizes approaching that of the core particle. These data indicate that the linker DNA attached to monomer fragments from sperm is more resistant to digestion than that of spermatid chromatin. The size for the core fragment determined here (150 bp) is larger than those of other eukaryotic chromatins.

Puigdomenech et al. (1987) have described a 151 bp particle

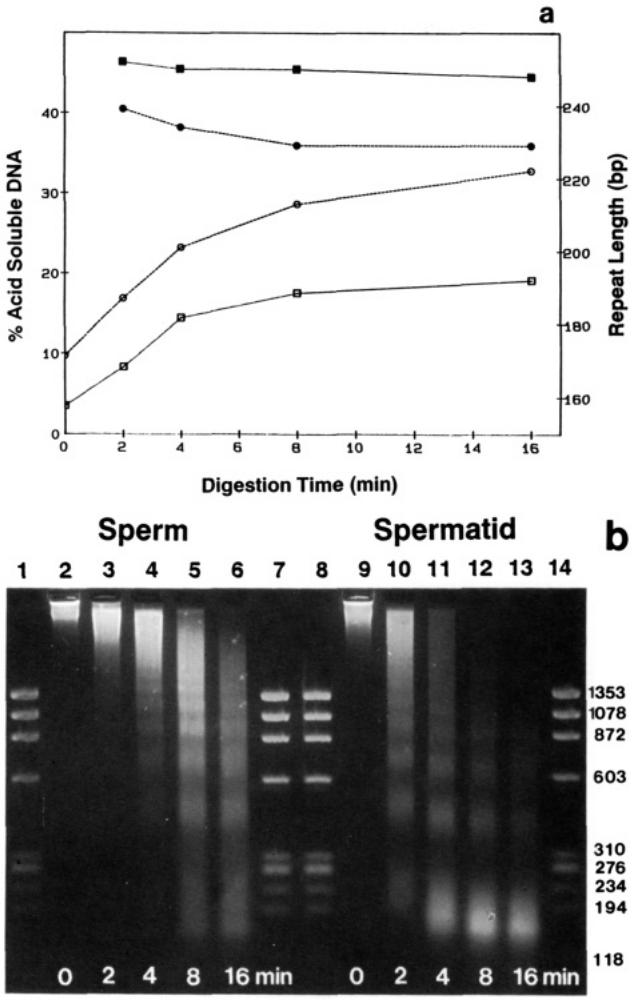

FIGURE 3: Digestion of sperm and spermatid chromatin with micrococcal nuclease. Sperm (□) and spermatid (○) chromatins, prepared from nuclei purified by Percoll centrifugation, were digested with micrococcal nuclease, and the amounts of DNA rendered soluble in acid were determined (a). DNA from the digests was purified and analyzed by electrophoresis on a 2% agarose gel, which was stained with ethidium bromide (b). Nucleosomal repeat lengths [sperm (■) and spermatid (●)] were determined from this gel and are recorded in (a). Lanes 1, 7, 8, and 14 contained ϕX174 DNA digested with *Hin*dIII restriction endonuclease. Sizes of restriction fragments in bp are indicated for lane 14. Lanes 2–6 contained sperm chromatin digested for 2, 4, 8, and 16 min with micrococcal nuclease, and lanes 9–13 contained spermatid chromatin digested for 2, 4, 8, and 16 min with micrococcal nuclease.

from extensively digested sea urchin sperm chromatin and attributed its large size to protection of the DNA by the globular domain of Sp H1 histone. Simpson and Bergman (1980) have reported a typical core of 146 bp.

In summary, both repeat length and rate of micrococcal nuclease digestion of spermatid chromatin are more like embryonic (somatic) than sperm chromatin. In addition, the unusual physical properties of sperm chromatin are acquired well after sperm histones have completely replaced somatic variants.

Thermal Denaturation. Spermatid and sperm chromatins at equivalent concentrations were thermally denatured in 0.25 M EDTA. First-derivative plots of the thermal denaturation curves are shown in Figure 4. Sperm chromatin melted almost entirely in two steps with midpoints of 65 and 82 °C, representing approximately one-third and two-thirds of the chromatin, respectively (Figure 4a). Since 40% (100 of 250 bp) of sperm DNA resides in the linker region of the chromatin, at least some of the linker DNA resides in the most stable

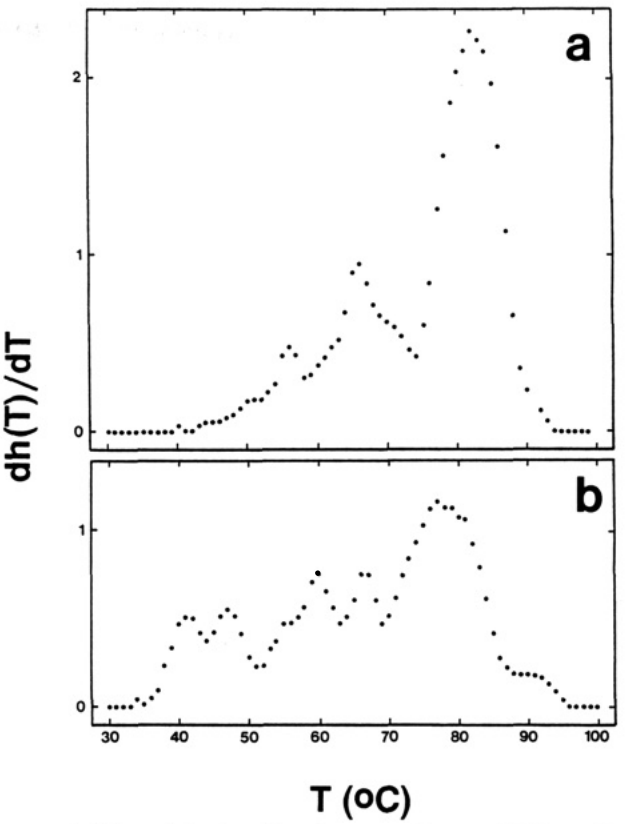

FIGURE 4: Thermal denaturation of sperm and spermatid chromatin. Sperm (a) and spermatid (b) chromatins, prepared from nuclei purified by Percoll centrifugation, were denatured by increasing the temperature in a water-jacketed cuvetted chamber at 0.5 °C/min while monitoring the absorbance at 260 nm. The starting absorbance of the samples was 0.5 at 260 nm, and the hyperchromicities for sperm and spermatid chromatin were 36% and 31%, respectively. Turbidity, measured at 320 nm, remained below 4% of the initial 260-nm absorbance of the samples throughout the course of denaturation.

fraction. In spermatid chromatin (Figure 4b), a much smaller fraction of the DNA (48%) melted at a high transition point (T_m = 78 °C, slightly lower than in sperm), and a significant fraction of the DNA melted below the lowest sperm transition.

Therefore, during spermatid differentiation, at least 20% of the DNA shifts to the highest melting fraction. The spermatid denaturation curve more closely resembles an embryonic than a sperm pattern (Ozaki, 1971). The elevated thermal stability of sperm chromatin is not simply a consequence of Sp histone variant substitution for somatic subtypes.

Discussion

Several distinctive features of sea urchin sperm chromatin have long been recognized. Sea urchin sperm is thermally stable (Ozaki, 1971), it has the longest known nucleosomal repeat length (Spadafora et al., 1976), and two of its five histones, Sp H1 and Sp H2B, are substantially larger than their somatic counterparts primarily because of extensions at their N-termini (Strickland et al., 1978, 1980).

After fertilization, Sp H1 and Sp H2B are specifically phosphorylated (Poccia et al., 1981; Green & Poccia, 1985), and the repeat length of the chromatin subsequently declines to somatic levels within the first cell cycle (Savič et al., 1981). Those observations led to a model for male pronuclear chromatin decondensation (Green & Poccia, 1985) incorporating some features of previous models of echinoderm sperm chromatin structure (Zalenskaya et al., 1981; Von Holt et al., 1984). The model has two central implications: strong ionic binding of Sp H1 and Sp H2B arms to linker DNA in mature sperm and decreased affinity of the arms for linker as a

consequence of histone phosphorylation following fertilization (Green & Poccia, 1985; Poccia, 1987).

It was more recently demonstrated that the phosphorylated forms of Sp H1 and Sp H2B are present throughout spermatogenesis, until the transition from late spermatid to mature sperm (Poccia et al., 1987). We proposed that sperm histone variants function in the phosphorylated state as normal somatic histones, when their arms are "neutralized" by phosphorylation. If this is the case, the acquisition of the long repeat length should occur late in spermatogenesis, and the resulting linker should be expected to be thermally stable and more resistant to digestion as a consequence of binding Sp N-terminal arms, rather than due to substitution of Sp variants for somatic variants.

In this study, we have used two probes of chromatin structure, micrococcal nuclease digestion and thermal denaturation, to test the predicted interactions of the N-terminal arms of Sp H1 and Sp H2B with linker DNA. Micrococcal nuclease preferentially attacks linker DNA (Noll & Kornberg, 1977), and thermal denaturation profiles are dominated by ionic binding between positive charges of histones and negative charges of the DNA sugar–phosphate backbone (Ansevin, 1982). For example, H1-depleted chromatin shows increased micrococcal nuclease sensitivity and decreased thermal stability (Allan et al., 1980; Kaplan et al., 1984). Sea urchin sperm chromatin is more resistant to micrococcal nuclease digestion and thermal denaturation than embryonic chromatin, but these chromatins differ substantially in histone variant composition (Ozaki, 1971; Arceci & Gross, 1980; Simpson & Bergman, 1980).

The results presented in this paper show that, in comparison with sperm chromatin linker DNA, spermatid linker is less resistant to digestion with micrococcal nuclease. Second, in spermatid chromatin, DNA is in a thermally less stable state, suggesting that weaker interactions of the basic histones with DNA occur. In these properties as well as repeat length, spermatid chromatin resembles typical chromatin from differentiated tissues of late embryo or adult. However, since spermatid and sperm chromatins contain identical histone variants, which differ in their phosphorylation state, rather than different histone subtypes, and since linker DNA is increased approximately 16 bp in sperm, we propose that dephosphorylation and subsequent interaction of Sp H1 and Sp H2B arms with linker DNA account for the changes in linker stability and sensitivity attained during spermiogenesis.

The simplest interpretation of the set of chromatin structural transitions observed is the following. Sometime during spermiogenesis, possibly in the late spermatid when sperm histones are dephosphorylated (Poccia et al., 1987), nucleosomal spacing is readjusted. Extra linker DNA characteristic of the mature sperm is then available for binding to the dephosphorylated highly basic arms of the Sp H1 and Sp H2B histones. These bind by strong ionic interactions, creating linker of high thermal stability and increased resistance to micrococcal nuclease.

Why might these structural changes be restricted to the last steps of spermiogenesis? Binding of the nonconserved portions of the sperm histones might be incompatible with normal chromatin function in the early proliferating cells of the male germ cell lineage as previously suggested (Poccia et al., 1987). We favor the idea that the arms are designed to function in the mature sperm cell and that they function only when able to strongly bind to DNA. The timing of the dephosphorylation and structural transitions suggests a role in the dense packaging of chromatin in the mature sperm cell. There are two ways that Sp histones might contribute to higner order chromatin structure by binding to linker DNA. Links may occur within chromatin fibers (short-range interactions) or between chromatin fibers (long-range interactions). Each has been suggested (Von Holt et al., 1984; Green & Poccia, 1985). Since the chromatin fibers in sea urchin sperm nuclei are essentially close packed (Green & Poccia, 1985), long-range interactions are feasible.

A long-range cross-linking function for the Sp H1 and H2B histone arms remains to be established, as does a role in stabilizing the extreme DNA compaction in the mature sperm nucleus. It is of interest, however, that in a computer search of the Protein Identification Resource data base (Georgetown University) for the peptide sequence characteristic of the Sp H1 and H2B histone arms (Ser-Pro adjacent to two basic amino acids), the only non-H1 proteins which showed multiple occurrences of the tetrapeptide were sea urchin Sp H2B, galline (chicken sperm basic protein), nucleocapsid protein of caronavirus, and core antigens of three hepatitus viruses (Poccia, 1987). More recently, wheat germ H2A was reported to contain three occurrences of the tetrapeptide (Rodriques et al., 1985). Each of these proteins is a nucleic acid binding protein associated with highly condensed nucleic acid which presumably decondenses following fertilization, germination, or infection. It is tempting to speculate that these proteins undergo similar phosphorylation/dephosphorylation mechanisms in control of chromatin packaging.

ACKNOWLEDGMENTS

We thank Dr. Dennis Searcy for assistance with the thermal denaturation studies and Marcia Simpson for helpful discussions.

REFERENCES

Allan, J., Staynov, D. Z., & Gould, H. (1980) *Proc. Natl. Acad. Sci. U.S.A. 77*, 885–889.
Ansevin, A. T. (1978) *Methods Cell Biol. 28*, 397–414.
Arceci, R., & Gross, P. (1980) *Dev. Biol. 80*, 186–209.
Busslinger, M., & Barberis, A. (1985) *Proc. Natl. Acad. Sci. U.S.A. 82*, 5676–5680.
Green, G. R., & Poccia, D. L. (1985) *Dev. Biol. 108*, 235–245.
Green, G. R., Searcy, D. G., & DeLange, R. J. (1983) *Biochim. Biophys. Acta 741*, 251–257.
Kaplan, L., Bauer, R., Morrison, E., Langan, T., & Fasman, G. (1984) *J. Biol. Chem. 259*, 8777–8785.
Keichline, D., & Wassarman, P. (1977) *Biochim. Biophys. Acta 475*, 139–151.
Kennedy, B. P., & Davies, P. L. (1982) *J. Biol. Chem. 257*, 11160–11165.
Lai, Z., & Childs, G. (1986) *Nucleic Acids Res. 14*, 6845–6856.
Lieber, T., Weisser, K., & Childs, G. (1986) *Mol. Cell. Biol. 6*, 2602–2612.
Louie, A. J., & Dixon, G. H. (1972) *J. Biol. Chem. 247*, 7962–7968.
Noll, M., & Kornberg, R. (1977) *J. Mol. Biol. 109*, 393–404.
Ozaki, H. (1971) *Dev. Biol. 26*, 209–219.
Poccia, D. (1986) *Int. Rev. Cytol. 109*, 1–65.
Poccia, D. (1987) in *Molecular Regulation of Nuclear Events in Mitosis and Meiosis* (Schlegel, R. A., Halleck, M. S., & Rao, P. N., Eds.) pp 149–177, Academic Press, New York.
Poccia, D. L., & Green, G. R. (1986) *Methods Cell Biol. 27*, 153–174.
Poccia, D. L., Greenough, T., Green, G. R., Nash, L., & Erickson, J. (1984) *Dev. Biol. 104*, 274–286.

Poccia, D. L., Simpson, M. V., & Green, G. R. (1987) *Dev. Biol. 121*, 445–453.
Puigdomenech, P., Romero, M. C., Allan, J., Sautiere, P., Giancotti, V., & Crane-Robinson, C. (1987) *Biochim. Biophys. Acta 908*, 70–80.
Rodrigues, J., Brandt, W., & Von Holt, C. (1985) *Eur. J. Biochem. 150*, 499–506.
Savič, A., Richman, P., Williamson, P., & Poccia, D. (1981) *Dev. Biol. 78*, 3706–3710.
Simpson, R. T., & Bergman, L. W. (1982) *J. Biol. Chem. 255*, 10702–10709.
Simpson, M. V., & Poccia, D. L. (1987) *Gamete Res. 17*, 131–144.
Spadafora, C., Bellard, M., Compton, J., & Chambon, P. (1976) *FEBS Lett. 69*, 281–285.
Strickland, M., Strickland, W., Brandt, W., Von Holt, C., Wittman-Liebold, B., & Lehmann, A. (1978) *Eur. J. Biochem. 89*, 443–452.
Strickland, W. N., Strickland, M., Brandt, W. F., Von Holt, C., Lehmann, A., & Wittmann-Liebold, B. (1980) *Eur. J. Biochem. 104*, 567–578.
Von Holt, C., de Groot, P., Schwager, S., & Brandt, W. F. (1984) in *Histone Genes* (Stein, G. S., Stein, J. L., & Marzluff, W. F., Eds.) pp 65–104, Wiley, New York.
Zalenskaya, I., Pospelov, V., Zalensky, A., & Vorob'ev, V. (1981) *Nucleic Acids Res. 9*, 473–487.

Investigations of the Partial Reactions Catalyzed by Pyruvate Phosphate Dikinase†

Hsuei Chin Wang,‡ Lawrence Ciskanik,‡ Debra Dunaway-Mariano,*,‡,§ Wolfgang von der Saal,‖ and Joseph J. Villafranca*,‖

Department of Chemistry and Biochemistry, University of Maryland, College Park, Maryland 20742, and Department of Chemistry, The Pennsylvania State University, University Park, Pennsylvania 16802

Received June 5, 1987; Revised Manuscript Received August 18, 1987

ABSTRACT: The kinetic mechanism of pyruvate phosphate dikinase (PPDK) from *Bacteroides symbiosus* was investigated with several different kinetic diagnostics. Initial velocity patterns were intersecting for AMP/PP_i and ATP/P_i substrate pairs and parallel for all other substrate pairs. PPDK was shown to catalyze [^{14}C]pyruvate ⇄ phosphoenolpyruvate (PEP) exchange in the absence of cosubstrates, [^{14}C]AMP ⇄ ATP exchange in the presence of P_i/PP_i but not in their absence, and [^{32}P]P_i ⇄ PP_i exchange in the presence of ATP/AMP but not in their absence. The enzyme was also shown, by using [$\alpha\beta$-^{18}O,β,β-$^{18}O_2$]ATP and [$\beta\gamma$-^{18}O,γ,γ,γ-$^{18}O_3$]ATP and ^{31}P NMR techniques, to catalyze exchange in ATP between the $\alpha\beta$-bridge oxygen and the α-P nonbridge oxygen and also between the $\beta\gamma$-bridge oxygen and the β-P nonbridge oxygen. The exchanges were catalyzed by PPDK in the presence of P_i but not in its absence. These results were interpreted to support a bi(ATP,P_i) bi(AMP,PP_i) uni(pyruvate) uni(PEP) mechanism. AMP and P_i binding order was examined by carrying out dead-end inhibition studies. The dead-end inhibitor adenosine 5′-monophosphorothioate (AMPS) was found to be competitive vs AMP, noncompetitive vs PP_i, and uncompetitive vs PEP. The dead-end inhibitor imidodiphosphate (PNP) was found to be competitive vs PP_i, uncompetitive vs AMP, and uncompetitive vs PEP. These results showed that AMP binds before PP_i. The ATP and P_i binding order was studied by carrying out inhibition, positional isotope exchange, and alternate substrate studies. The dead-end inhibitor adenylyl imidodiphosphate (AMPPNP) was shown to be noncompetitive vs P_i, which ruled out an ordered mechanism in which P_i binds first. The positional isotope exchange rates observed with [$\alpha\beta$-^{18}O,β,β-$^{18}O_2$]ATP as a function of P_i concentration followed a normal saturation curve, eliminating an ordered mechanism in which ATP binds first. The initial velocities of the PPDK-catalyzed reaction of P_i and of the two alternate substrates arsenate and thiophosphate were measured as a function of ATP concentration. A Lineweaver–Burk plot of these data indicated a random mechanism. Product inhibition studies were carried out by using initial velocity and equilibrium isotope exchange techniques. The results from these studies indicate that the ATP/P_i and AMP/PP_i binding steps are at steady state and that AMP forms an abortive complex. Two possible chemical mechanisms are described, one of which involves the intermediacies of a covalent pyrophosphoryl-enzyme and a covalent phosphoryl-enzyme and the other of which involves the intermediacies of ADP and a covalent phosphoryl-enzyme.

Pyruvate phosphate dikinase (PPDK)[1] catalyzes the reversible phosphorylation of pyruvate and inorganic phosphate by a single molecule of ATP: pyruvate + ATP + P_i ⇄ PEP + AMP + PP_i. The enzyme has been found in the amoeba *Entamoeba histolytica* (Reeves, 1960), in the leaves of C_4 plants (Hatch & Slack, 1968), and in a variety of bacteria (Evans & Wood, 1968; Reeves et al., 1968; Buchanan, 1974;

† This work was supported by NSF Grant PCM-8409737 to J.J.V. and NIH Grants GM 28688 and GM 36260 to D.D.-M.
* Author to whom correspondence should be addressed.
‡ University of Maryland.
§ NIH Career Development Awardee (ES 00111) and Alfred P. Sloan Fellow.
‖ The Pennsylvania State University.

[1] Abbreviations: PPDK, pyruvate phosphate dikinase; PEP, phosphoenolpyruvate; NMR, nuclear magnetic resonance; HPLC, high-pressure liquid chromatography; SDS–PAGE, sodium dodecyl sulfate–polyacrylamide gel electrophoresis; FPLC, fast protein liquid chromatography; TLC, thin-layer chromatography; HEPES, *N*-(2-hydroxyethyl)piperazine-*N*′-2-ethanesulfonic acid; PIPES, piperazine-*N*,*N*′-bis(2-ethanesulfonic acid); EDTA, ethylenediaminetetraacetic acid; AMPS, adenosine 5′-monophosphorothioate; PNP, imidodiphosphate; AMPPNP, adenylyl imidodiphosphate; PIX, positional isotope exchange; Tris, tris(hydroxymethyl)aminomethane; TCA, trichloroacetic acid; AMPPCP, adenylyl methylenediphosphate; AMPCPP, adenosine 5′-(α,β-methylenetriphosphate).

0006-2960/88/0427-0625$01.50/0